

# Reactive Alloys of IIA Metals: Gas Sorption and Corrosion as One Process

Konstantin Chuntonov<sup>1\*</sup> , Alexey O. Ivanov<sup>2</sup>, Viktor L. Kozhevnikov<sup>3</sup>

<sup>1</sup>NanoShell Consulting, Migdal Haemek, Israel

<sup>2</sup>Department of Theoretical and Mathematical Physics, Ural Federal University, Yekaterinburg, Russia

<sup>3</sup>Institute of Solid State Chemistry, Russian Academy of Sciences, Yekaterinburg, Russia

Email: \*konstantin@chuntonov.com

**How to cite this paper:** Chuntonov, K., Ivanov, A.O. and Kozhevnikov, V.L. (2021) Reactive Alloys of IIA Metals: Gas Sorption and Corrosion as One Process. *Journal of Materials Science and Chemical Engineering*, 9, 39-69.  
<https://doi.org/10.4236/msce.2021.911004>

**Received:** October 8, 2021

**Accepted:** November 27, 2021

**Published:** November 30, 2021

Copyright © 2021 by author(s) and Scientific Research Publishing Inc. This work is licensed under the Creative Commons Attribution International License (CC BY 4.0).

<http://creativecommons.org/licenses/by/4.0/>



Open Access

## Abstract

The present work summarizes the results of previously known, as well as the latest sorption measurements, which were carried out on IIA metal alloys in the form of films, powders and macrobodies with a monolithic structure. Analysis of these data made it possible to construct an empirical sorption model, according to which the corrosive decomposition of reactive alloys is one of the driving forces of the sorption process. This model provides a qualitative description of the sorption behavior of these alloys in a gas environment and can be useful in solving practical problems in the field of vacuum and gas technologies.

## Keywords

Gas Sorption, Corrosion, Getters, Triboreactors, Vacuum Windows

## 1. Introduction

Alkaline earth metals and their alloys actively trap gases at ambient temperatures, forming non-volatile chemical compounds. In the capturing of gases, not only the surface is involved here, but also the volume, which explains the multiple superiority of these alloys in specific sorption capacity over other gas sorbents [1] [2] [3] [4] [5]. Let us note also that IIA metals are widespread in the earth's crust, and their production does not require high costs. All this stimulates the development of sorption technologies based on these metals.

Meanwhile, the experience of the very first steps in this direction shows that all those techniques and norms that were proposed and built earlier for adsorbents are not applicable to IIA metals due to their high reactivity [6]. This reactivity creates serious problems if one follows the generally accepted practice for

adsorbents of dispersing the sorbent material and then transferring it to the working position. In the case of IIA metal alloys, it is clear that a different organization of the sorption process and other sorption equipment are required [7] [8].

For example, in the field of gas purification, triboreactors with alloy IIA metal ingots [9] [10] claim to replace the usual sorption columns with getters adsorbents [11] [12] [13]. Such a replacement promises unprecedented consequences for sorption technologies: controlled kinetics of this process, simplification of sorption equipment, minimization of costs for the production of purification material, as well as reaching the theoretical limit for specific sorption capacity.

The prospects for IIA metal alloys are no less promising in the field of vacuum technologies, where a high sorption capacity of the getter material is a priority requirement. This is especially true in the case of vacuum windows with thermal insulation [5] [14], vacuum MEMS devices [15], vacuum insulated pipes, etc. The deficiency of internal space in such chambers forced the search for an alternative to mechanical activation, and the corrosive decomposition of reaction ingots was used [10] [14] as such an alternative.

The driving force of sorption in this case is the destruction of the structure of the ingot by the very gases that are to be captured. The initial body of the alloy decomposes in the course of corrosion into fragments and particles, which separate from it and in this way increase the area of the surface accessible to gases by orders of magnitude in comparison with the initial one. The law, according to which the ingot disintegrates, is pre-set at the stage of its casting and during post casting treatment [14], when the microstructure of the ingot is formed, and defects are formed and allocated in its body.

An analysis of the experimental data accumulated to date on the behavior of IIA metal alloys in a gaseous medium under isothermal conditions is given below. Our goal is to build a preliminary picture of the interaction between gases and these materials, which we named getters reactants in accordance with [16].

## 2. Getters Reactants

The ability of alkaline earth metals and their alloys to capture large amounts of gases is well known [1] [2] [3] [4] [5] [17] [18] [19] [20] [21]. This process is based on a chemical reaction, and its products are compounds in which there can be several gas atoms per metal atom. For example, these can be not only oxides, hydrides, nitrides and other binary compounds, but also more complex ones, such as hydroxides, IIA metal salts, etc.

Such an advantageous quantitative ratio between the sorbing material and the gas in the products of their interaction is unthinkable when adsorbents are used, no matter how large their specific surface area is. Even hypothetically, none of the carcass structures such as zeolites or MOFs (metal organic frameworks) [22] [23] [24] [25] [26] is capable of approaching such a ratio, especially since there is also a mandatory requirement for these structures to have the necessary reserved me-

chanical strength. Moreover, getters adsorbents of the NEG type (non-evaporable getters) based on transition metals cannot compete with alloys of IIA metals [3] [5] [21] [27] [28].

The question of the production cost of the considered sorbents, adsorbents, on the one hand, and getter reagents, on the other, is also clear. While adsorbents are highly porous, gas-permeable bodies that must be activated before starting the sorption process, getter reagents are conventional ingots of IIA metal alloys, ready for direct use.

Let us also consider the question of time dependence of characteristics of an isothermal sorption process with the participation of getters reactants. It is known from experience that in air, cast samples of IIA metals and their alloys are quickly covered with a layer of products that slow down the sorption process. It is this behavior of getters reactants that is recorded in the experimental curves of the sigmoid shape  $\Delta m(t)/m$  (Figure 1), obtained using the weight method in the ordinary atmosphere [10] [14]. Here  $m$  is the initial mass of the getter reactant, found by weighing it in air,  $\Delta m(t)$  is the current mass gain (mass of the captured gas), and  $t$  is time.

Usually, several minutes pass before measurements start and during this time the samples are covered with a layer of products that slow down the further course of the process. This time delay in gas sorption appears on the graph as an almost horizontal segment  $0-t_d$  (Figure 1). At this stage (stage I), the reactant is practically not consumed, which can be used for practical purposes. However, after the point  $t_d$ , the reaction of the gas with the alloy resumes and goes into the mode of an intensive sorption process (stage II). In the end, having passed point  $t_f$  the reaction reaches stage III, exceeding any adsorbents in specific sorption capacity by many times.

## 2.1. The Chemical Reaction as a Sorption Process

The chemisorption of gases by IIA metals, as mentioned above, is not limited only to the surface, but goes deeper, capturing the volume of the material. Mostly such processes were studied on films [1] [2] [20] [29] [30] [31] [32], and not

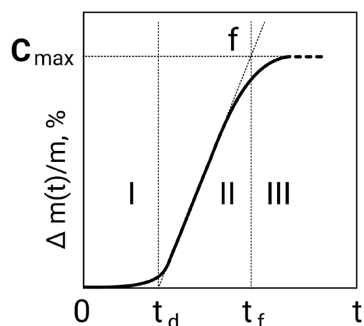


**Figure 1.** General view of the sorption curve of getters reactants in air [10]. I—sorption pause, II—intensive sorption stage, III—the end of the sorption process;  $m$  is the initial mass of the sample,  $\Delta m(t)$  is the current mass gain,  $t$  is the time.

on bulk monolithic bodies. In those cases, when the object of study was monolithic bodies or the products of their coarse grinding, the procedure of sorption measurements was stopped as soon as the sorption rate decreased by about 100 times compared to the initial one [21] [27] [28].

Such actions of the authors of these works are explained by the recommendations of the ASTM [33], but they turned out to be incorrect when applied to reactive monolithic bodies. Therefore, the results of works [21] [27] [28] are not final and need to be reconsidered. At first glance, the data [21] [27] [28], obtained by the dynamic sorption method, and the data [10] [14], obtained by the weight method, have little in common. However, **Figure 2** puts everything in its place, combining both groups of these data.

Indeed, a 100-fold decrease in the rate of sorption of getters reactants, contrary to the position of ASTM [33], is not the evidence of the end of the sorption process, but only indicates a temporary respite in the reaction of the gas with the ingot. This sorption pause indicates the transition of the ingot to the state of “quasi-passivation”, when the cover layer of the reaction products reaches a certain critical thickness  $\Delta h$ , which temporarily stops the reaction of the gas with the metallic surface. As is shown in **Figure 1**, at the end of the  $0-t_d$  segment, the  $\Delta m(t)/m$  curve revives and rises to the point  $f$ , demonstrating high sorption capacity of the reactive alloys [10] [14].

The curves  $\Delta m(t)/m_0$  in **Figure 2**, as well as the curve  $\Delta m(t)/m$  (**Figure 1**), were built up by the weighing method, but here  $m_0$  is the mass of a fresh sample weighed in a glove box under argon still before the contact with air. Immediately after this, the balance and the sample of the reactant were taken out and all further measurements continued in the ordinary atmosphere. This gives us the right to interpret the curve  $\Delta m(t)/m_0$  as a result of adding together two

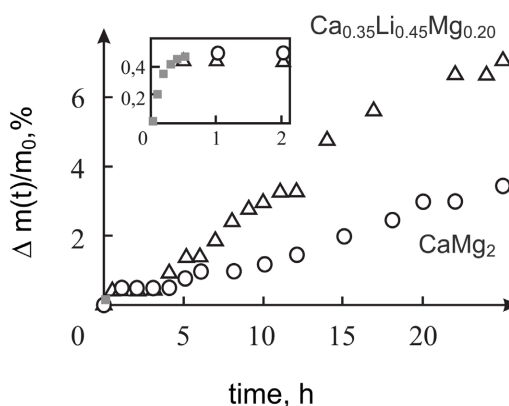


**Figure 2.** Sorption curves  $\Delta m(t)/m_0$  with the stage of growth of the cover layer of products  $\Delta h$ . The measurements were carried out on samples of the mass from 0.200 g to 0.600 g with weighing accuracy of  $\pm 0.001$  g. The size of the symbols on the graphs fully included the measurement error. Gray points are the averaged results of [21] [27] [28].

successive parts of a single sorption process, the formation of a cover layer of products in air and subsequent sorption phenomena described by the curve  $\Delta m(t)/m$  (Figure 1). In other words, in Figure 2, the nearest to the origin of coordinates horizontal segment corresponds to the sorption pause  $0-t_d$  shown in Figure 1, and the initial branch of the curve from point (0,0) to this horizontal segment corresponds to the growth of the cover layer (gray dots).

The question of “sewing together” the data [21] [27] [28] with the data [10] [14] can be solved by estimating the thickness of the covering layer of the products  $\Delta h$  in both cases. As can be seen from Figure 2, a sorption pause occurs here at a level of about 0.5% along the ordinate  $\Delta m(t)/m_0$ . Since the average linear size of the samples  $d$  was  $\sim 5$  mm, according to the calculation method [10] [14], we get a value of  $\sim 4.2$   $\mu\text{m}$  for the thickness of the covering layer.

The results obtained from the data [21] [27] [28] are close to this. Thus, based on the data [27] [28], we come to the conclusion that particles of a barium alloy with a size from 1 to 4 mm by the end of measurements are covered with a layer of products with a thickness of 4 to 7  $\mu\text{m}$ , and following the measurement data [21], where particles of Ba alloys reached a size  $\sim 0.25$  mm, we arrive at the value  $\Delta h \sim 5$   $\mu\text{m}$ .

This closeness of the  $\Delta h$  values obtained using different measurement techniques gives the ground to generalize the shape of the  $\Delta m(t)/m_0$  curves (Figure 2), taking them as a typical graphic image of all those processes, in which the countdown of the mass of the sample begins from the initial value of  $m_0$ . In [21] [27] [28], the cover layer  $\Delta h$  was formed during the time from several minutes to several tens of minutes, but under the conditions when the pressure of the gas phase was by five orders of magnitude lower than atmospheric. Therefore, the data of these works after transferring to Figure 2 describing the processes in air turn into an almost vertical fragment of the curve near the ordinate axis (gray dots).

The  $\Delta m(t)/m_0$  curve is close in shape to the well-known  $\alpha(t)$  curves (Figure 3), describing heterogeneous reactions of the gas-solid type [34] [35]

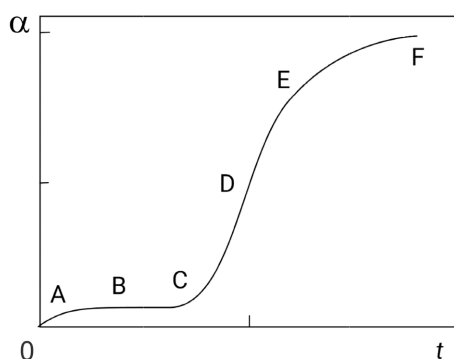


**Figure 3.** Typical  $\alpha(t)$  curve of a heterogeneous reaction [36].  $\alpha$ —reaction yield,  $t$ —time;  $A$ —initial stage,  $B$ —incubation period,  $C$ —acceleration period,  $D$ —inflection point,  $E$ —decay period,  $F$ —reaction completion.

[36], where  $\alpha$  is the reaction yield and  $t$  is time.

This similarity of the curves  $\alpha(t)$  and  $\Delta m(t)/m_0$  looks quite expected due to the close nature of the described processes – isothermal heterogeneous reactions, and it manifests itself both in an extended horizontal segment at the incubation stage of the process and in the subsequent rise of the curves. Let us try to rely upon this analogy, not forgetting about the features of IIA metals.

Experiments show (Figure 1 and Figure 2) that the reaction of gases with IIA metal alloys does not end after a 100-fold decrease in sorption kinetics in gas/reactive ingot systems. On the opposite, like in the case of the  $\alpha(t)$  curve, where the incubation stage B (Figure 3) passes over time into the acceleration stage C, the  $\Delta m(t)/m_0$  curve also, after a certain calm period on the horizontal segment of the curve, demonstrates a sharp revivification of the interaction between the gas and the ingot, exceeding the level of the incubation stage in the reaction yield by more than an order of magnitude (Figure 2).

This behavior of getters reactants in a gaseous medium does not follow either from the classical theory of metal oxidation [37] [38] [39] [40], or from the latest theories of adsorption kinetics [41] [42] [43], where both of them are limited to the analysis of processes on the surface. Figure 4 and Figure 5 with their clear illustration of the corrosive decomposition of samples of  $\text{Li}_2\text{Sr}_3$  and  $\text{Ca}_{0.7}\text{Mg}_{0.3}$  in air at room temperature indicate the emergence of a new participant in the sorption process. This picture of the apparent structural destruction of the alloy under the influence of atmospheric gases is so convincing that we only have to take one step—to build a bridge between such branches of solid state chemistry as the kinetics of heterogeneous reactions and corrosion of metals in a gas environment, thereby expanding the boundaries of our analysis.

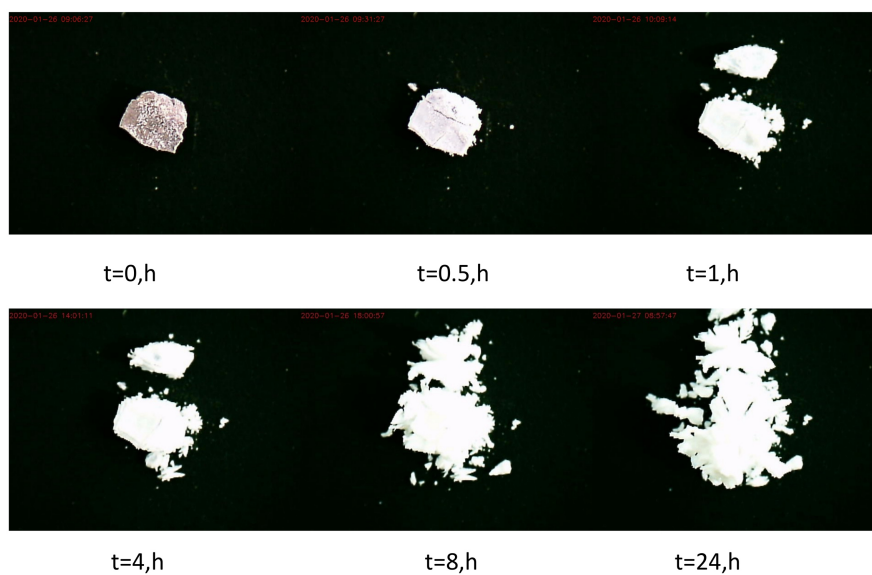


**Figure 4.** Corrosion decomposition of the  $\text{Li}_2\text{Sr}_3$  intermetallic compound in air. Micrographs of a particle with mass  $m = 0.201$  g. According to chemical analysis, the reaction products are oxides and nitrides of alloy components.

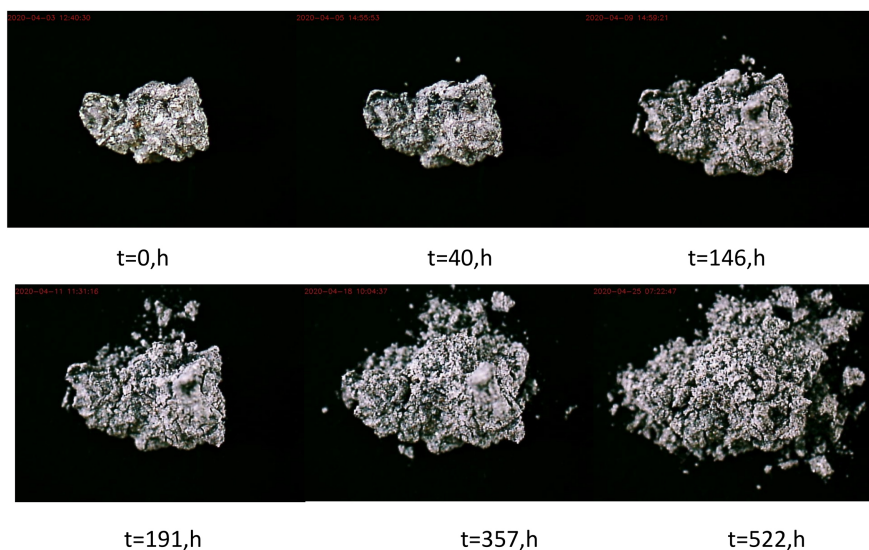


**Figure 5.** Corrosion decomposition of the  $\text{Ca}_{0.7}\text{Mg}_{0.3}$  eutectic alloy in air. Micrographs of a particle with mass  $m = 0.414$  g. According to chemical analysis, the reaction products are oxides of alloy components.

The role of ingot disintegration in the appearance of an inclined part of the  $\Delta m(t)/m$  curve between points  $t_d$  and  $t_f$  is obvious (**Figure 1**). This decay becomes a generator of a fresh surface, feeding the reaction in the gas/ingot system with new areas of the metal surface at the places of ingot fracture. A new situation arises with clearly positive prospects for sorption applications. Let us consider the mechanism of this disintegration in order to see how we can influence the disintegration of the ingot and with it the kinetics of the sorption process.

## 2.2. Corrosion Decomposition as a Sorption Process

**Figure 6** schematically shows a cross section of a cast sample of IIA metals alloy, where 1 is the surface of the alloy, 2 are microcracks, and 3 are grain boundaries. These three structural elements of the ingot serve as a chemical sink for atmospheric gases, each with its own mechanism of interaction.

Let's start with the surface 1. As soon as the alkaline-earth metal alloy comes into contact with atmospheric gases, it begins to be covered (in full accordance with the Pilling-Bedworth criterion [39] [40]) with a loose layer of reaction products, which makes it difficult for gases to directly access the metal surface (**Figure 6(b)**). In this case, the transport of gases through this slowing, but not insulating layer becomes the limiting stage of the sorption process.

By the time when the sorption rate decreases by about two orders of magnitude, the thickness  $\Delta h$  of the product layer reaches a value of several microns [10] [14] and this moment can be taken for a conditional start of the incubation stage, which goes on up to the point  $t_d$  (**Figure 1**). The length of this stage depends both on the chemical nature of the gas/alloy pair and on the degree of development of the structural elements of ingot 2 and 3 (**Figure 6(a)**).

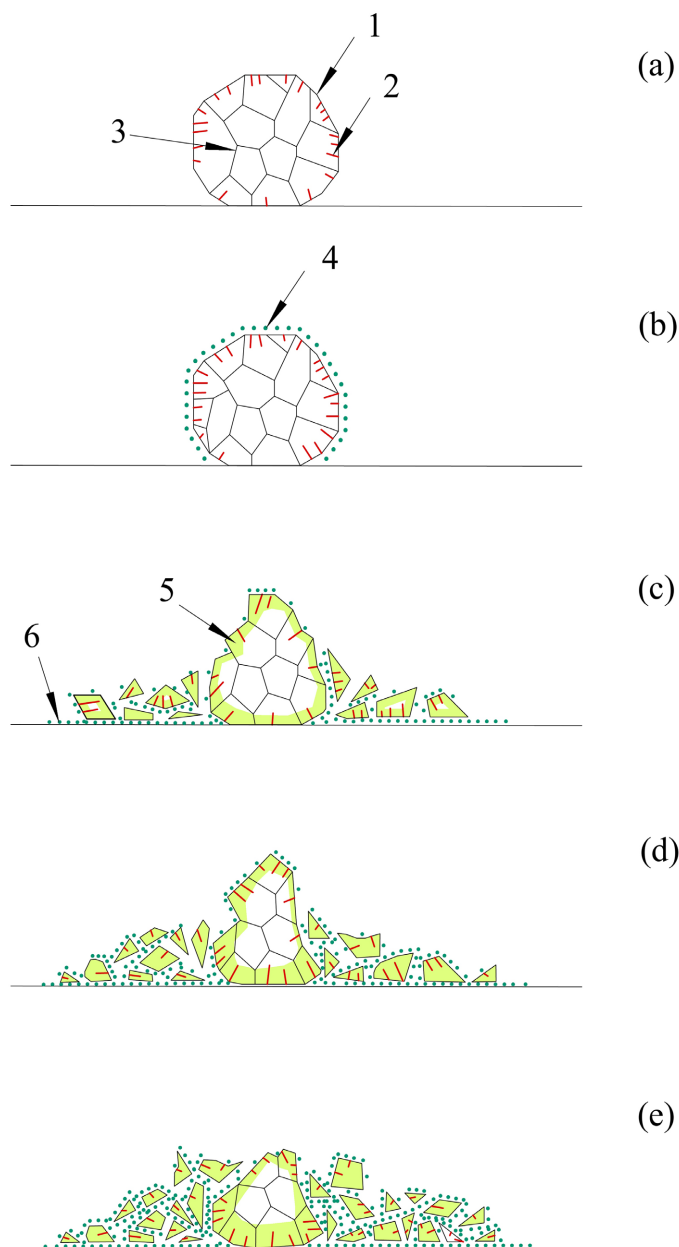


**Figure 6.** Chemisorption process together with corrosive decomposition of the reactive ingot. 1—ingot surface, 2—micro-cracks, 3—grain boundaries, 4—slowing layer  $\Delta h$ , 5—zone of gas occupation, 6—a scree of reaction products; (a) at the starting state, (b) at the stage of incubation, (c)-(e) successive stages of corrosion destruction of the ingot, assisted by the sorption process.

The processes of gas capturing by microcracks 2, intercrystalline boundaries 3 and surface 1 start simultaneously. However, the rate of filling the microcracks with gases and the rate of their diffusion along the intercrystalline boundaries are relatively low, in particular, due to the small area of the inlet section of these sinks, when compared with the total surface area of the ingot. And yet, it is these structural elements 2 and 3 that are responsible for the sharp rise in the

$\Delta m(t)/m$  curve after the point  $t_d$  (Figure 1). However, their influence on the sorption rate is realized through mechanical destruction of the ingot.

As is known, the growth of microcracks in the presence of tensile stresses and an aggressive medium has an intermittent character [44] [45] [46]. Until a local embrittlement zone is formed in front of the crack tip, there is no noticeable crack movement. However, with the appearance of such a zone, a rapid destruction of the material occurs within this zone. Then these actions are repeated and repeated until a complete fracture of the sample with its falling into separate parts takes place. This last phase of the ingot decomposition is accompanied by the appearance of a noticeable region of fresh surface.

A stepwise shape is inherent in all sorption curves  $\Delta m(t)/m$  of reactive alloys at the stage of their corrosion decomposition. As an example, let us point out the sorption curves of the alloys  $\text{Ca}_{0.35}\text{Li}_{0.45}\text{Mg}_{0.20}$  and  $\text{Ca}_{0.56}\text{Li}_{0.20}\text{Mg}_{0.24}$  shown in Figure 7 and Figure 8, respectively.

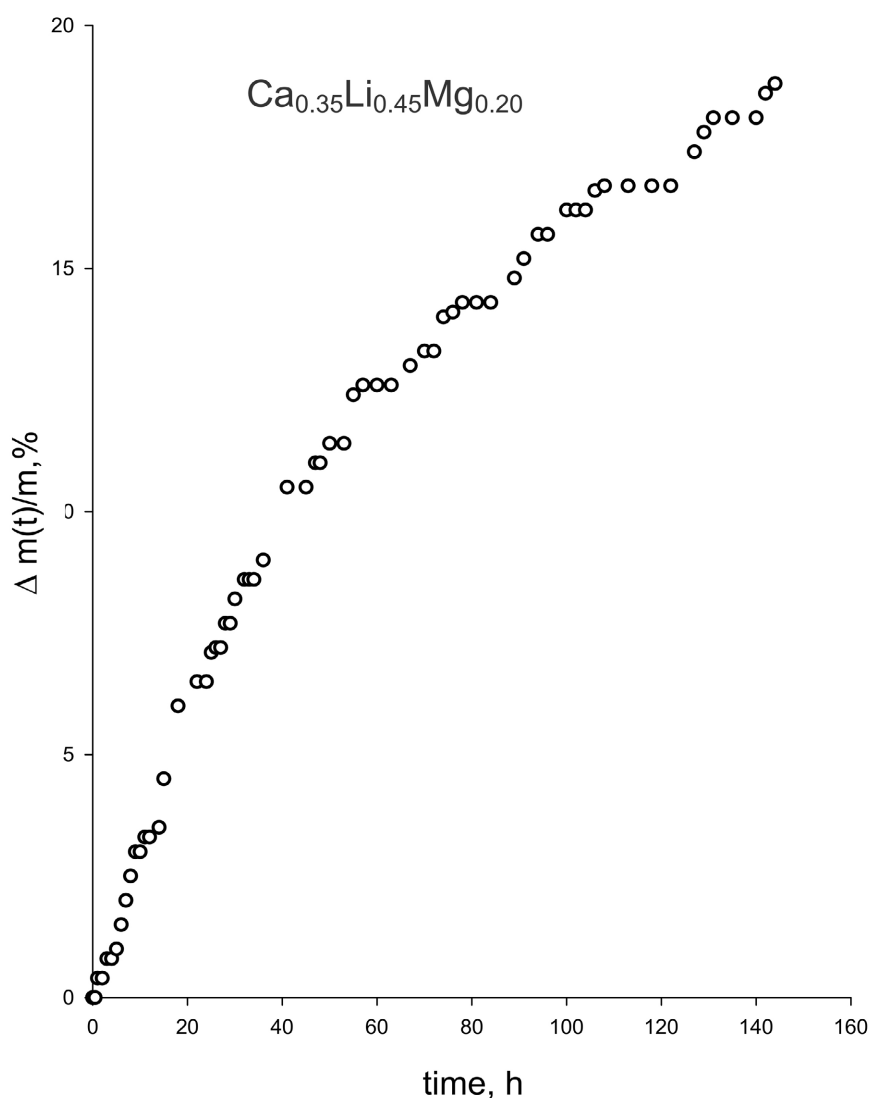
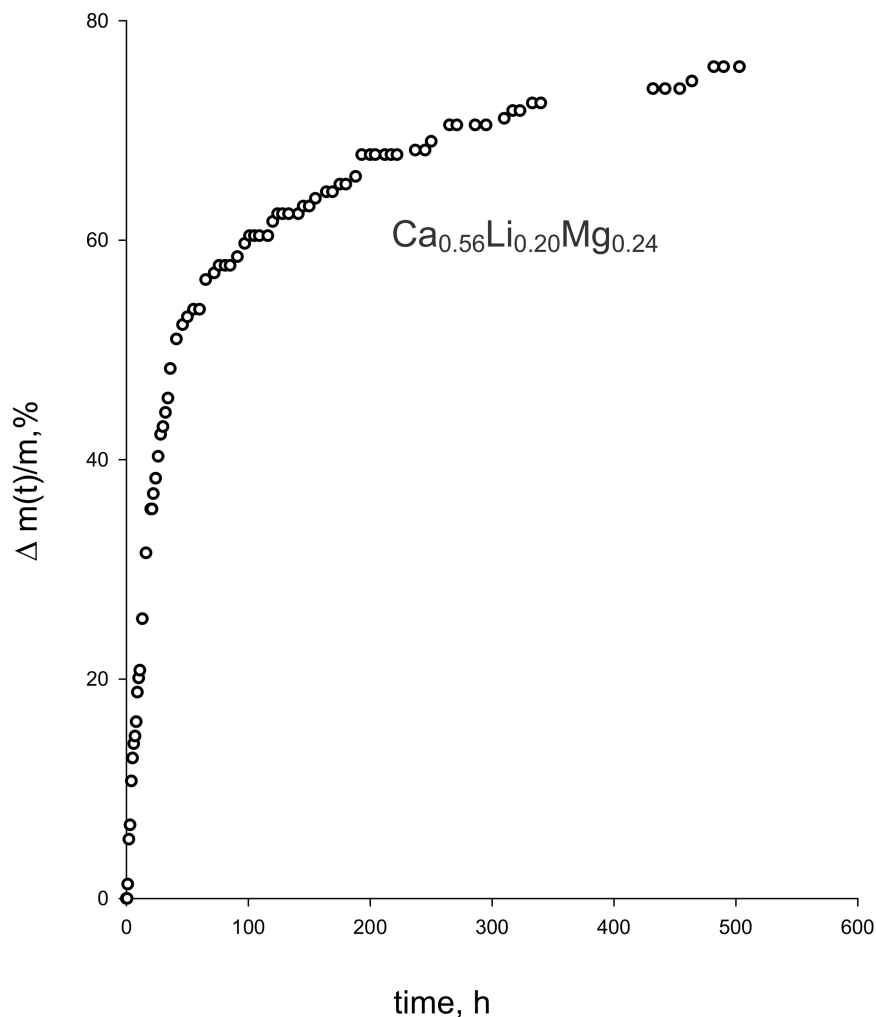


Figure 7. Sorption curve of the ternary alloy  $\text{Ca}_{0.35}\text{Li}_{0.45}\text{Mg}_{0.20}$  under normal conditions.



**Figure 8.** Sorption curve of the ternary alloy  $\text{Ca}_{0.56}\text{Li}_{0.20}\text{Mg}_{0.24}$  under normal conditions.

In the same cases, when the sorption curve looks smooth, such as the curves of the intermetallic phase  $\text{CaMg}_2$  in **Figure 11**, **Figure 13**, it is enough to increase the scale of values along the ordinate axis and then the step-like nature of this curve is immediately manifested (**Figure 9**).

Each curve  $\Delta m(t)/m$  is the sum of the sorption effects produced by all those cracks that originate, grow and end their life as a fracture during measurements in the tested sample. The horizontal segments of these curves, *i.e.*, steps, are those states when all microcracks in the sample are in the incubation stage, and sharp jumps from step to step are associated with the intensive growth of the sorption layer on that fresh surface that appears as a result of the corresponding fracture.

**Figure 6(a)** shows that whatever the geometry of the residual forces in the sample is, there will always be a sufficient number of surface microcracks, which are oriented perpendicular to these forces or some of their components. In our case, there is also a second necessary condition for the development of microcracks, this is the embrittlement of their walls due to chemical reactions between

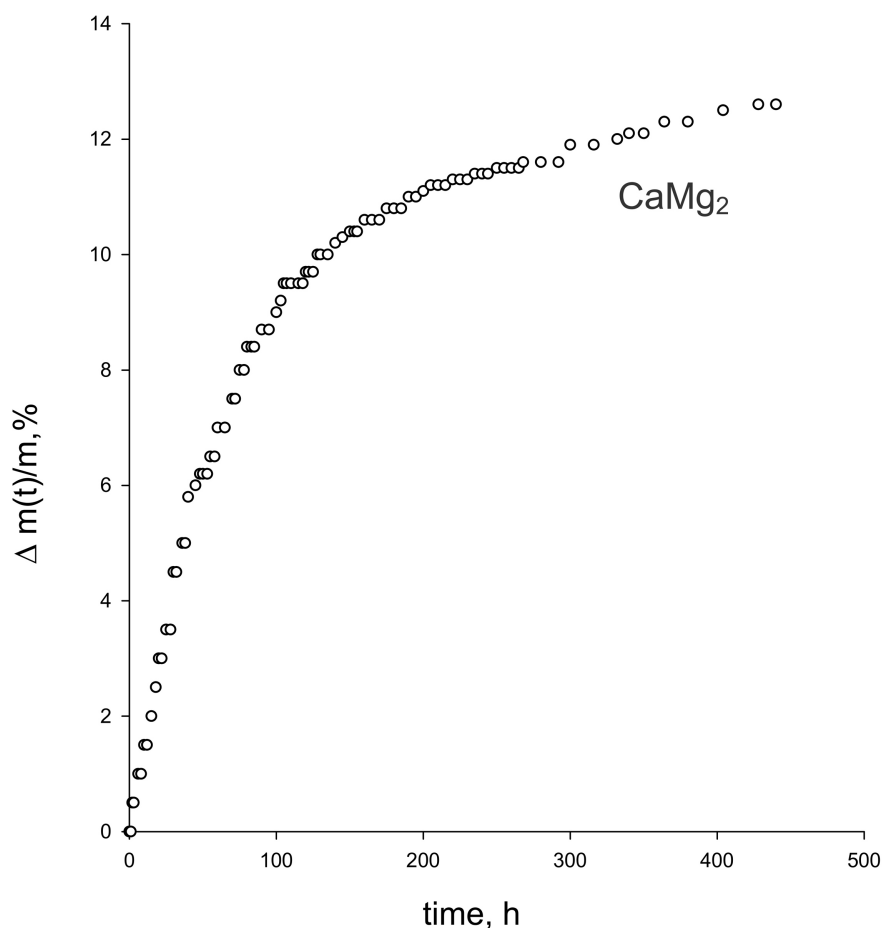


**Figure 9.** Sorption curve of intermetallic  $\text{CaMg}_2$  under normal conditions.

the metal and gases entering the crack.

One of the efficient ways of filling microcracks with gases is their capillary condensation, e.g., condensation of water vapor or water together with carbon dioxide. This condensate reacts with IIA metals, which leads to hydrogen embrittlement of the material surrounding the crack tip and to additional pressure on the walls of the microcracks. Such consequences were observed in the case of magnesium alloys repeatedly [47] [48] [49], and the accelerated destruction of cast getters reactants under the influence of moisture was also recorded in our experiments (**Figure 10**).

The third chemical sink for gases is intergranular boundaries 3 in the ingot (**Figure 6(a)**). Here, the alloy undergoes a gas attack through the boundaries, which, as a result of the reaction with gases, lose their metallic nature; and this leads to a sharp decrease in the cohesion forces among the grains. Accordingly, the ability of the reactive material to withstand tensile stresses weakens and this brings the time of its destruction closer. The effect of intercrystalline corrosion decomposition on gas sorption by getters reactants is shown in **Figure 11** and **Figure 12**.

The sorption curves of the  $\text{Ca}_{0.7}\text{Mg}_{0.3}$  eutectic and the intermetallic compound

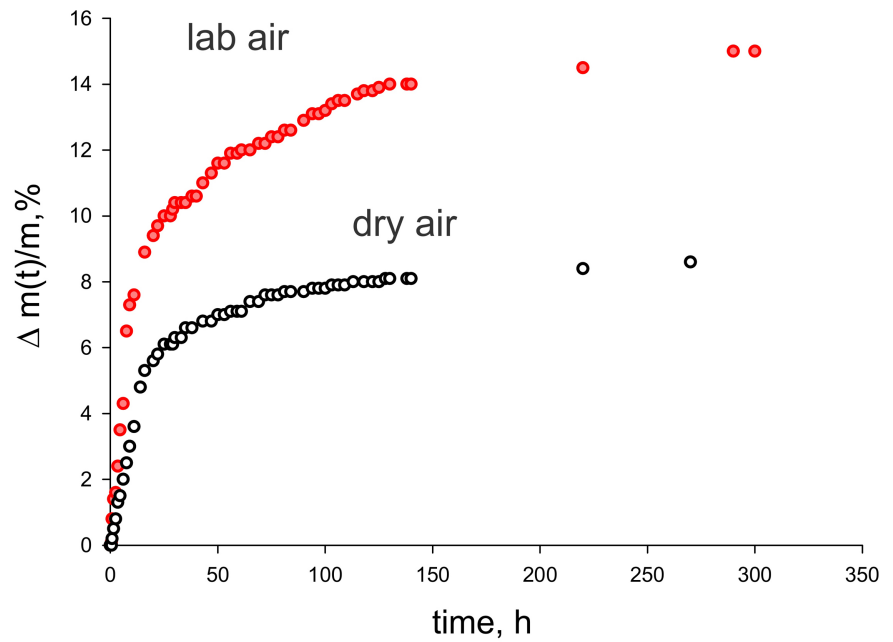


**Figure 10.** Sorption curves of the ternary alloy  $\text{Ca}_{0.35}\text{Li}_{0.10}\text{Mg}_{0.55}$  under normal conditions and in a dry atmosphere.

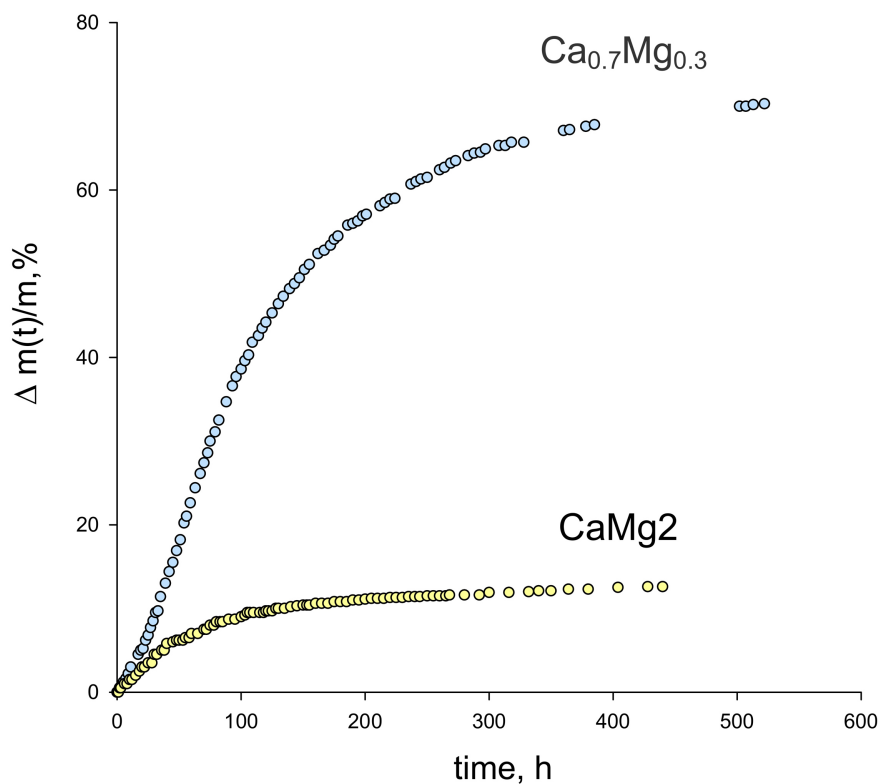


**Figure 11.** Sorption curves  $\Delta m(t)/m$  for Ca alloys with Mg:  $\text{Ca}_{0.7}\text{Mg}_{0.3}$  eutectic vs  $\text{CaMg}_2$  intermetallic compound.

$\text{CaMg}_2$  with a coarse-grained structure, are compared in **Figure 11**, and the sorption curves of the  $\text{CaLi}_2$  intermetallic compound in its two forms,

coarse-grained and fine-grained, are compared in **Figure 12**. It can be seen that in both cases the samples of the material with a developed network of intercrystalline boundaries have a noticeable superiority in sorption kinetics.

### 2.3. Lithium and Its Role

The most active of the IIA metals, barium, is toxic and therefore undesirable in many alkaline earth metal applications. If we exclude barium from the composition of getters reactants, then lithium is a good substitute for it. In this case, four metals become the element base of getters reactants: Mg, Ca, Sr and Li, where lithium can be used both as an alloying metal and as a base metal. Unlike other alkali metals, lithium easily alloys with IIA metals in any proportions, forming with them solid solutions, eutectics, and intermetallic compounds [50]. Also, lithium is not inferior to IIA metals in chemical activity, and reacts with gases to the end under normal conditions as well [51] [52] [53] [54].

A striking illustration of the influence of the chemical factor on the sorption process is **Figure 13** with its sorption curves  $\Delta m(t)/m$  for the intermetallic compounds  $\text{Li}_2\text{Sr}_3$  and  $\text{CaMg}_2$ . It can be seen that after a 14-hour exposure of the samples in an ordinary atmosphere, the first of them managed to capture a gas mass 100 times greater than the second one. Here we see not only the higher activity of strontium than that of Ca and Mg, but also the ability of lithium to accelerate the corrosive decomposition of the reactant.

Confirmation of this role of lithium can be found in **Figure 14** and **Figure 15**. It can be seen that the addition of lithium to the intermetallic phase  $\text{CaMg}_2$  as well as to the eutectic  $\text{Ca}_{0.7}\text{Mg}_{0.3}$  accelerates the decay of both of them.

Presumably, the course of the sorption process in these cases can be described

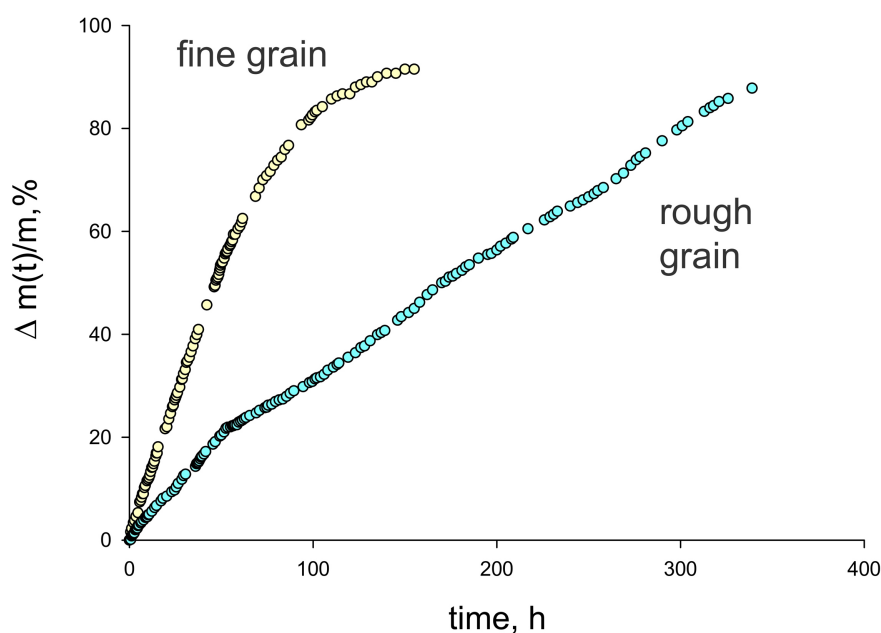


**Figure 12.** Sorption curves  $\Delta m(t)/m$  for intermetallic  $\text{CaLi}_2$ : coarse-grained structure vs fine-grained structure.

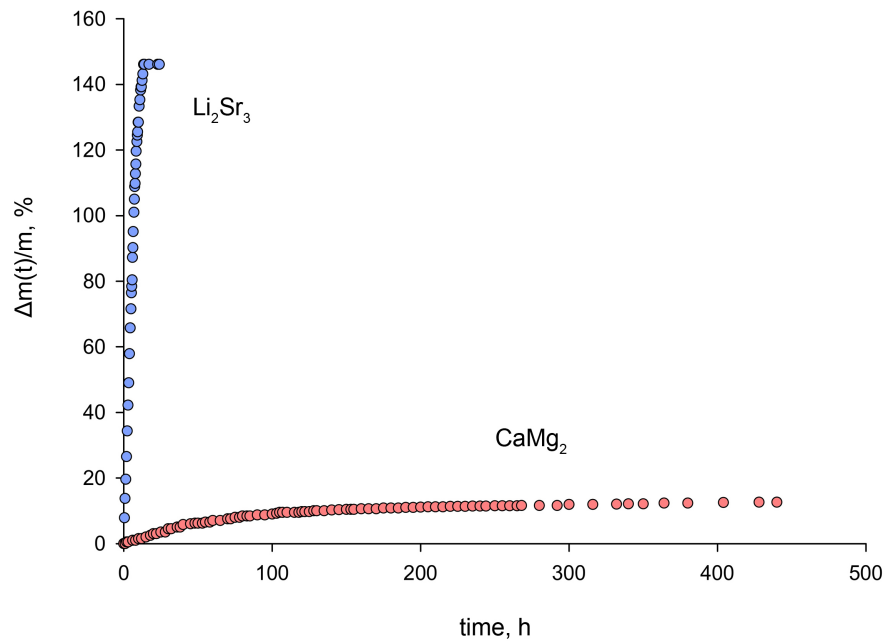


**Figure 13.** Effect of a chemical factor on the sorption process: intermetallic  $\text{Li}_2\text{Sr}_3$  vs intermetallic  $\text{CaMg}_2$ .

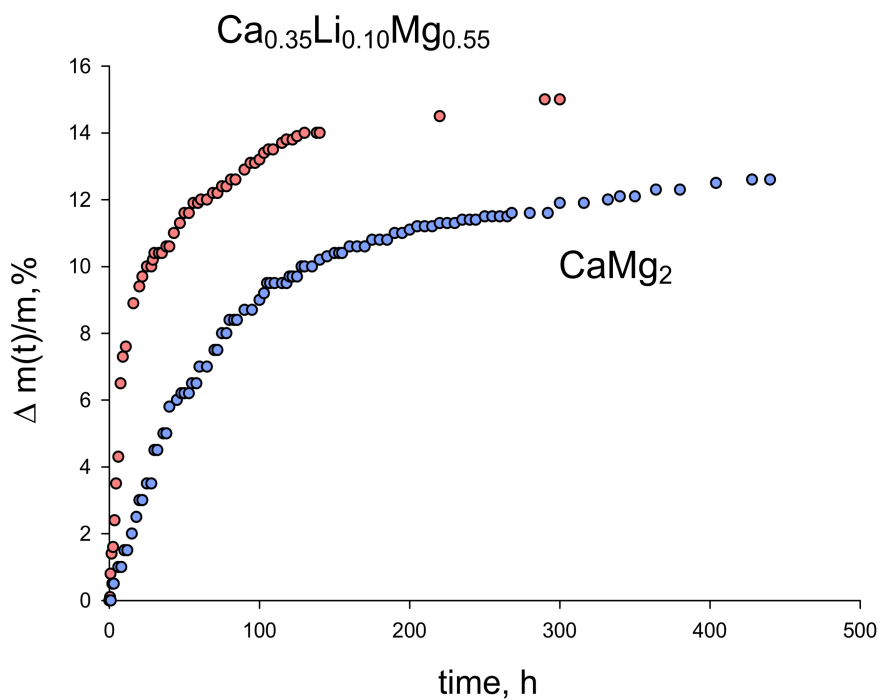


**Figure 14.** Effect of lithium on the rate of corrosion decomposition: ternary alloy  $\text{Ca}_{0.35}\text{Li}_{0.10}\text{Mg}_{0.55}$  vs intermetallic  $\text{CaMg}_2$ .

as follows. When gases fill microcracks or penetrate into the boundaries separating the ingot grains, the lithium atoms present in the crystal lattice of the grains are the first to leave their positions and diffuse into the places of gas accumulation, where the reaction takes place. This activity of lithium is explained in particular

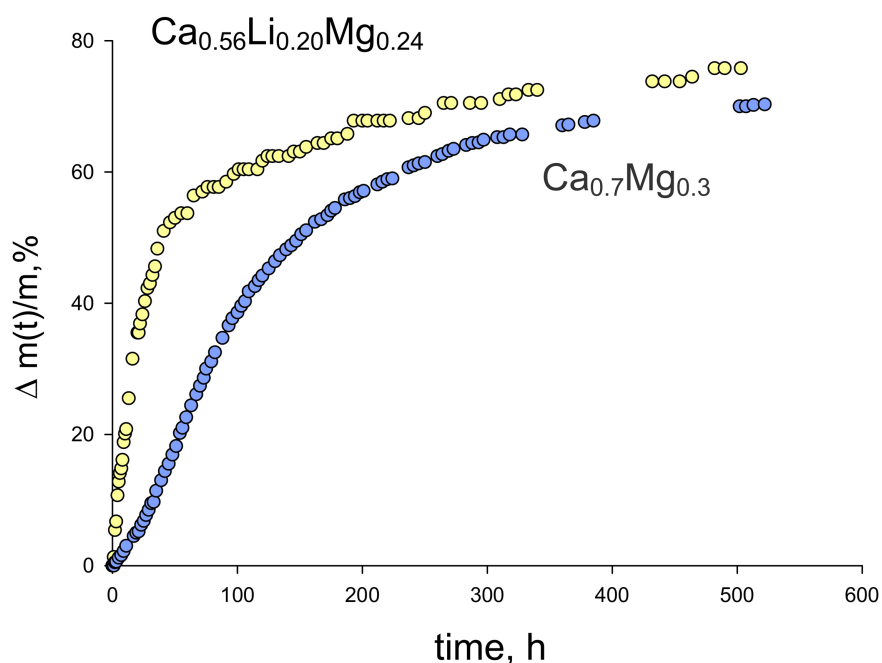


**Figure 15.** Effect of lithium on the rate of corrosion decomposition: ternary alloy  $\text{Ca}_{0.56}\text{Li}_{0.20}\text{Mg}_{0.24}$  vs  $\text{Ca}_{0.7}\text{Mg}_{0.3}$  eutectic.

by the relatively small size and high mobility of its atoms.

When lithium atoms leave the bulk of the grains, vacancies appear in them, while in the reaction zone, where the gases are located, new products are formed, which increases the pressure on the walls from the inside. These two events contribute to the destruction of the crystalline body, accelerating the sorption process.

### 3. Empirical Process Model

Let us try to generalize these new facts with those known earlier in order to obtain a unified picture of the sorption behavior of reaction alloys in atmospheric gases under normal conditions. As can be seen from the above, the similarity of the curves  $\Delta m(t)/m_0$  and  $\alpha(t)$  is somewhat violated by the step-like shape of the first ones at the post-incubation stage (Figure 2, Figures 7-9), while the curve  $\alpha(t)$  retains its smooth shape along the entire length (Figure 3). Let us also point out the differences in the processes described by the curves  $\Delta m(t)/m_0$  and  $\alpha(t)$ . For example, while the incubation stage B (Figure 3) is usually associated with the nucleation of a new phase, in the system gas/getter reactant it corresponds to the processes of filling the ingot with gases along intergranular boundaries and microcracks, which prepare the disintegration of the crystalline body.

Thus, the interaction of gases with getters reactants in isothermal conditions is not reduced to the known variants of heterophase reactions of the  $\alpha(t)$  type, despite the obvious relationship with them. Therefore, let us turn again to Figure 6 and consider consecutively the entire chain of events occurring with an

ingot in a gaseous medium.

The amount  $\Delta m$  of gas sorbed by the surface 1 (**Figure 6(b)**) during the first minutes of the exposure of the sample to air can be estimated using the expression  $\Delta m = kS\Delta h$ , where  $S$  is the surface area of the sample,  $\Delta h$  is the thickness of the slowing layer, and  $k$  is the coefficient characterizing the weight fraction of the gas per volume unit of the reaction products. Further growth of products due to reactions on the surface  $S$  is extremely small and manifests itself only in a slow growth of the slowing layer 4 and its exfoliation in the form of particles 6 in the vicinity of the sample (**Figures 6(c)-(e)**).

A new active stage of the sorption process begins after point  $t_d$  (**Figure 1**). The time interval  $0-t_d$  is the period of ripening of the ingot for its subsequent permanent decay in the segment between the points  $t_d$  and  $t_f$ . The attack of the alloy by gases can be represented as a frontal movement of a certain zone of gas occupation 5 (yellow area in **Figures 6(c)-(e)**) from the surface of the ingot to its center. Occupation here means the filling of microcracks and grain boundaries with gases with all the ensuing consequences (see Section 2.2).

Mechanical destruction of an ingot after point  $t_d$  consists of many individual acts of splitting and separation of various particles and fragments from its body. The rate of appearance of the cover layer on the surface of the fracture, as well as the rate of the act of destruction, is orders of magnitude higher than the kinetics of diffusion and migration processes within the material that occur in it at the incubation stage. The given ratio of these two kinetics is manifested in the stepped shape of the  $\Delta m(t)/m$  curves, which, as can be seen from **Figures 7-9**, consist of a sequence of horizontal segments that rise one after the other along the  $t$  axis.

Each segment of this kind is the next incubation stage, separated from neighboring segment by fracture acts, which are accompanied by an abrupt increase in the amount of gas  $\Delta m = ks\Delta h$  on the exposed clean surface of area  $s$ . According to the mentioned scheme, the sorption of the bulk of the gas occurs when the capture of gas by the getter reactant is localized within the narrow time vicinity of each fracture act. Immediately after such an act, the next incubation stage begins, the lifetime of which is incomparably longer than the time of the fracture. All these facts lead us to two fundamentally important conclusions that have both theoretical and practical significance for sorption technologies.

The first conclusion concerns sorption kinetics. It was shown above that this characteristic of getters reactants is completely limited by the kinetics of the phenomena that take place at the incubation stages of the entire sorption process. In essence, these are questions of the initiation and propagation of cracks inside a crystalline body.

The second conclusion refers to the specific sorption capacity. This characteristic of getters reactants in atmospheric gases at ambient temperature reaches its theoretical limit by the time when the initial ingot decays completely. In this context, complete disintegration means the situation when the average linear

size  $d$  of the products of corrosion destruction approaches twice the thickness of the slowing layer  $\Delta h$ . After that, the completion of the sorption process is a matter of just a few minutes.

The described picture of the interaction of monolithic samples of a reactive alloy with ambient gases forms a simple sorption model, the central place in which is taken by two processes, the formation of a slowing layer of products  $\Delta h$  on the surface of a solid and the subsequent corrosive decomposition of the ingot, which increases manifold the total area of the metal surface reacting with gases (**Figures 6(c)-(e)**).

Formally, this model is based on two terms, a slowing layer  $\Delta h$  and corrosive destruction of the material, including the thesis about the enormous kinetic superiority of processes on a metal surface over those in the bulk of an ingot. Meanwhile, the given model can also be presented graphically as a certain sequence of curves  $\Delta m(t)/m_0$ , which vary with changes in the structural elements of the ingot in question (**Figure 16**).

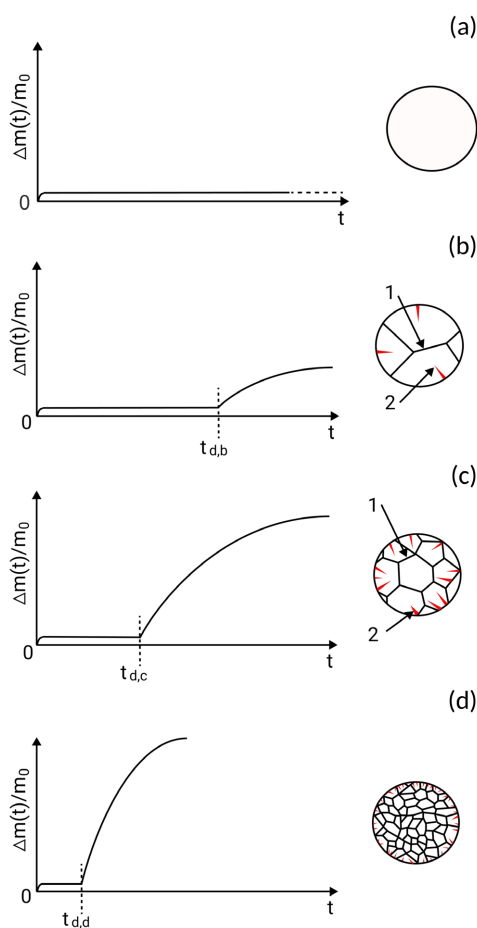


**Figure 16.** Graphic image of the sorption model. 1—boundaries between grains, 2—micro-cracks;  $t_{d,b}$ ,  $t_{d,c}$  and  $t_{d,d}$  are coordinates of the end of the incubation stage; (a) a single crystal, (b) a coarse crystal structure, (c) an ordinary polycrystal, (d) a fine-grained structure with a high concentration of defects.

With this approach, a clear relationship emerges between the structure of the alloy and its sorption behavior, which can be characterized by two quantities, the incubation pause  $0-t_d$ , which measures the resistance of the given alloy to air, and the slope of the sorption curve to the  $t$  axis, which measures the rate of gas sorption. This relationship helps to formulate and solve problems with adjusting the properties of the getter material to practical needs.

#### 4. Application Aspects

Let us summarize the intermediate results of our analysis, bearing in mind the sorption future of getters reactants. So, while adsorbents have a monolayer per unit of surface area, or, at best, several monolayers of adsorbate, in getters reactants, the  $\Delta h$  layer consists of several thousands of atomic layers. Such superiority of getters reactants could be compensated for by increasing the specific surface area of the adsorbents by the same thousands of times, but this is very difficult.

In the case of IIA metal alloys, from the very beginning, the general goal of the developments was seen in the implementation of such a scheme of the sorption process, where each atom of the getter material would take part in the chemical bonding of gases. The destruction of the initial structure of the reactive alloy by tribochemical methods [9] [10] [55] or corrosion decomposition [10] [14] leads to this very goal, providing getters reactants with an unconditional leadership among all sorbing materials in terms of specific sorption capacity.

According to experimental data [5] [21] [27], the specific sorption capacity of cast samples of the reactive material is not less than by  $\sim 100$  times higher than that of getters adsorbents of the NEG's type. Further exposure of such ingots or their fragments in a gas atmosphere increases this superiority by another factor of 20 - 100 [10] [14] [54]. This multiple increase in sorption capacity due to the corrosive decomposition of ingots is convincingly demonstrated in the above sorption curves (Figures 7-15).

Among other advantages of IIA metals and their alloys, we point out the simplicity of manufacturing their ingots in comparison with the long-term and multistage synthesis of gas-permeable porous adsorbents, both metallic (NEG's-type getters) and non-metallic (zeolites, MOFs). Equally important for applications is the incubation pause on  $\Delta m(t)/m$  curves, which greatly simplifies such important production operations as the assembly of vacuum chambers or the loading of sorption columns with purification material in air.

A cover layer of the thickness  $\sim 5 \mu\text{m}$  equates reactive cast materials with conventional materials when performing auxiliary operations in air. By selecting the optimal shape and size of the reactive product, it is possible to minimize its loss at the stage of introduction into the workplace [9] [10] [14]. Thus, in the case of 1 mm thick plates or ribbons of getter material, these losses do not exceed 1% of the initial mass, and in the case of bulk cylindrical ingots with a diameter of  $\sim 2$  cm, the losses decrease to 0.1%.

The sorption model described in Section III can also provide some assistance in solving sorption problems. In accordance with it, any reactive alloy of a set composition can be associated with its graphic image of the type shown in **Figure 16**, a sort of its “personal passport”. With a change in the composition of the alloy, something in this “passport” changes, but not the general law of the behavior of this alloy. This law is that an increase in the number of microcracks on the surface of an ingot and/or a decrease in the grain size inevitably leads to a decrease in the incubation time and to an increase in the sorption rate (**Figures 16(a)-(d)**). The mentioned regularity endows this model with an operational function that prompts the steps for improving the working characteristics of the getter material.

The practical interest in the length of the incubation stage and in the slope of the sorption curve in the region after the point  $t_{d,i}$  ( $i = a, b, c, d$ ) is quite understandable. As mentioned above, the horizontal segment  $0-t_{d,i}$  of the general curve is ideal for loading operations with a reactive alloy in air. This becomes possible if two values are coordinated with each other, the length of the segment  $0-t_{d,i}$  and the independent from it value of  $t_E$  equal to the real time spent on loading and hermetization of the reactor or vacuum chamber.

Not less important for practice is the slope of the sorption curve, which determines the gas sorption rate. Here it is necessary to bring two values closer together, the required sorption rate and that which the getter material is capable of. Taking into account the content of Section III, it is obvious that the advantages will be in the alloy with high reaction kinetics, *i.e.*, in fine-grained alloys with many structural defects (curve (d) in **Figure 16**).

The question of matching the values of  $t_{d,i}$  and  $t_E$  looks more complicated. Theoretically, two options are possible here, either  $t_{d,i} < t_E$  or  $t_{d,i} \geq t_E$ . If the first inequality holds, then some of the active material will be lost still at the loading stage. This is unacceptable and a way out of this situation is possible provided that the receiving party, *i.e.*, the developers or manufacturers of reactors or vacuum chambers, find a way to reduce the time  $t_E$  of the loading procedure at the expense of their technical resources.

The second option, that is, the ratio  $t_{d,i} \geq t_E$ , is completely acceptable. Moreover, it is possible to bring the values of  $t_{d,i}$  and  $t_E$  closer together if there is a large gap between them, using the chemical factor, *i.e.*, changing the alloy composition. **Figure 13** shows how strong the sorption effect can be with radical changes in composition, while **Figure 14** and **Figure 17** give an example of milder consequences.

#### 4.1. Chemical Composition of Getter Reactants

The data accumulated in the field of sorption studies show that the best material base for getters reactants is two-, three- and four-component alloys containing Ca, Mg, Sr, and Li. Two families of these alloys can be distinguished. One of them is alloys  $(Ca_xSr_{1-x})_yMg_{1-y}$ , where  $0 \leq x \leq 1$  and  $0.33 \leq y \leq 0.75$ , or the

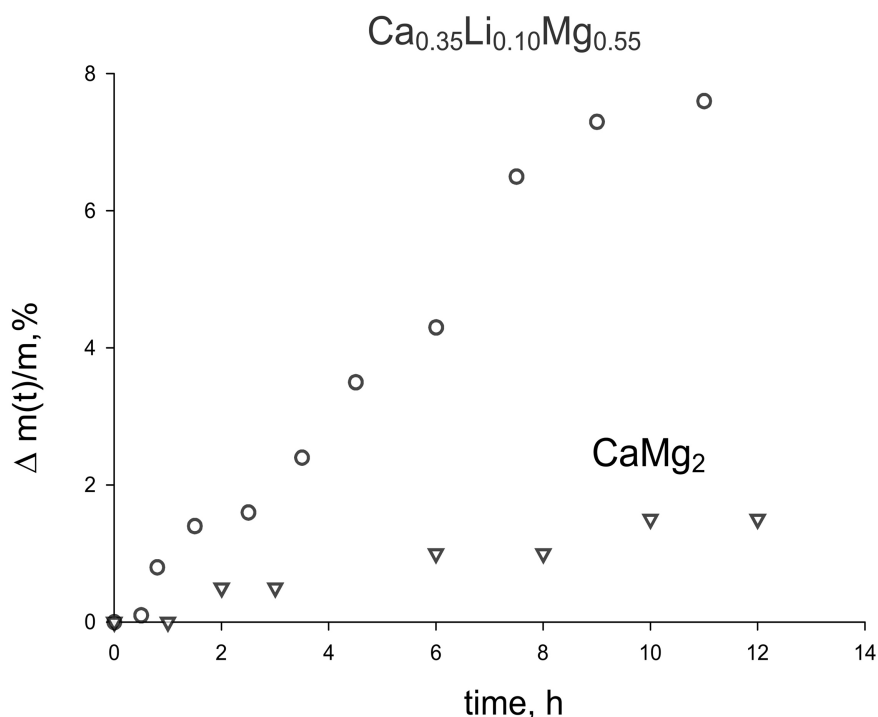


**Figure 17.** Effect of a chemical factor on the duration of the incubation stage: ternary alloy  $\text{Ca}_{0.35}\text{Li}_{0.10}\text{Mg}_{0.55}$  vs intermetallic  $\text{CaMg}_2$ .

same alloys, but alloyed with lithium. In **Figure 18** that part of the Ca–Mg–Sr ternary system [56] [57], which is part of this first family, is marked in yellow.

The given family of alloys fully satisfies the needs of gas purification technologies, providing a wide range of reactive alloys from monocrystalline bodies of variable composition  $(\text{Ca}_x\text{Sr}_{1-x})\text{Mg}_2$  to eutectic alloys of approximate composition  $(\text{Ca}_x\text{Sr}_{1-x})_y\text{Mg}_{1-y}$ , where  $0 \leq x \leq 1$  and  $0.65 \leq y \leq 0.75$ . In **Figure 18** this area of eutectic alloys is highlighted by hatching. On the whole, these alloys with Mg concentration from 25 to 67 at% give all the possibilities for efficient use of the sorption selectivity of alkaline earth metals.

In the case of vacuum technologies, where the main driving force of the sorption process is the corrosive decomposition of the ingot, the internal readiness of the material for destruction by gases is important. So here it is enough to restrict ourselves to the family of alloys with eutectic structure  $(\text{Ca}_x\text{Sr}_{1-x})_y\text{Mg}_{1-y}$  with  $0 \leq x \leq 1$  and  $0.65 \leq y \leq 0.75$ . The advantages of the eutectic are due to its developed network of grain boundaries and a special binary-phase microstructure, which serve as an active chemical sink for ambient gases. This structure of the ingot is the result of solidification of the melt, the composition of which belongs to a certain vicinity of the eutectic point in the phase diagram [58]. The solidification process in the case of interest to us consists of the usual steps for melting the initial charge, homogenizing the melt and cooling it. In terms of costs, considering, moreover, that all IIA metals melt below  $850^\circ\text{C}$ , this production is quite economical.

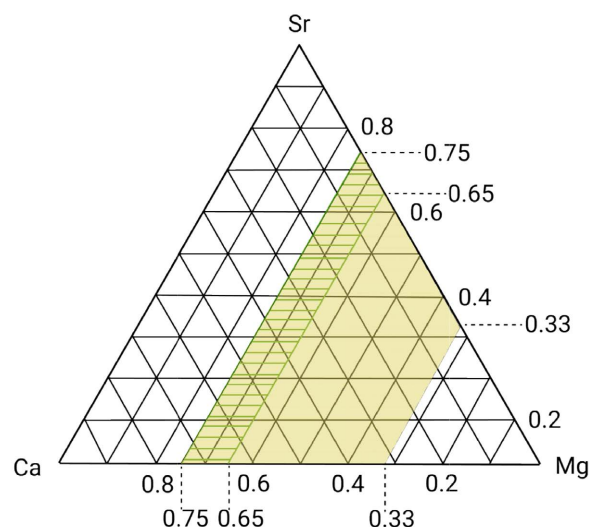


**Figure 18.** Preferred concentration limits for getters reactants. Yellow area—alloys for gas applications, shaded area—alloys for vacuum applications.

When applied to vacuum chambers, these eutectic alloys become one of the main pillars of the described technology, along with the two that have already been considered above, namely, with a slowing cover layer  $\Delta h$  on the surface of the ingots and with the corrosive decomposition of the alloy. This significance of the indicated eutectic is due not only to its developed microstructure, which increases the rate of decomposition of the alloy in gases, but also to its composition, which is characterized by a successful combination of the plastic solid solution  $\text{Ca}_x\text{Sr}_{1-x}$ , where  $0 \leq x \leq 1$ , and the brittle intermetallic phase  $(\text{Ca}_x\text{Sr}_{1-x})\text{Mg}_2$ .

By changing the shape of the mold and the temperature regime of solidification, it is possible to control the level of residual stresses in the reaction ingot, while additional mechanical treatment of these ingots by forging, cutting, rolling, etc., endows the final product with a special texture that expands its sorption capabilities in vacuum applications. The main task of the eutectic in vacuum applications is to ensure the disintegration of the ingot into particles with a characteristic size  $d \leq 2\Delta h$ .

## 4.2. Tribochemical Reactors

Mechanical activation of getters reactants in a gas environment expands the capabilities of sorption technologies. The design of the triboreactor can be very simple (**Figure 19**): a conventional high-pressure cylinder 1 with the processed gas, alloy ingots inside and a pressure gauge 3 attached to it is rotated around its longitudinal axis in a horizontal position.

The rotation of the cylinder 1 (**Figure 20**) sets the ingots 3 in motion, so that they are mutually grinded, freeing from the outer layers 4 that have reacted with the gas 2.

The continuously renewing alloy surface captures gases by orders of magnitude faster than a surface with a layer of reaction products. Let us pay attention

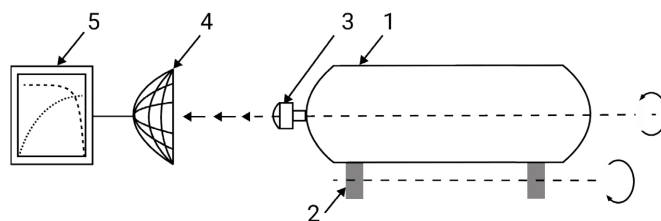


**Figure 19.** Rotating triboreactor with a pressure gauge [10]. 1—high pressure cylinder, 2—actuator, 3—pressure gauge, 4—signal receiver, 5—electronic converter.

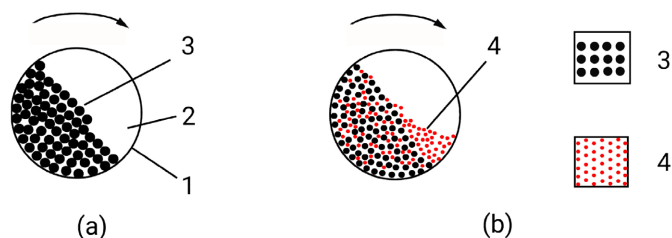


**Figure 20.** Gas purification in the process of autogenous grinding of cast getter particles. 1—cylinder wall, 2—processed gas, 3—getter material, 4—waste particles; (a) the beginning of the process, (b) the mode of “soft” grinding.

to two positive facts. The first is the dependence of the gas sorption rate on the number of cylinder revolutions per time unit, which makes the tribochemical method of gas treatment controllable. The second fact is the continuous monitoring of the state of the gas/ingot system thanks to the pressure gauge 3 (Figure 19).

The data on the gas pressure inside the cylinder is transmitted wirelessly to a remote receiver 4 with subsequent processing of the received signal by the converter 5 into the sorption characteristics of the process [10]. Both producers of pure gases and developers of sorbent materials are interested in this kind of information.

Tribochemical gas purification has a number of advantages over other gas purification technologies. Let us point out the simplicity of the equipment, low costs in servicing the purification process, and low costs in the production of reaction ingots. The energy consumption here is small at least because IIA metal alloys are mechanically fragile, the products of their reaction with gas are a brittle material with a loose structure, and the process of abrasion of ingots is also supported by their corrosive decomposition.

At the end of the purification process, the operation of separating the solid reaction products and gas is performed. The standard method uses metal filters, although other solutions are possible, such as bubbling a gas stream through an inert, non-volatile liquid, or using a centrifuge (centrifugal separator). The centrifugal separator is especially effective when purifying gases with low atomic mass, for example, when the final product of purification is hydrogen or helium.

However, a triboreactor with a pressure gauge can have other applications, in-

cluding serving as a tool for testing reactive alloys in various gas media with pressures ranging from vacuum to hundreds of bar. The results of such studies can deepen our knowledge of the mechanical activation of solids, which in the case of IIA metal alloys turns out to be not so much a source of high-energy excitation of the material as a generator of a fresh sorbing surface.

An important application of tribo-reactors with getters reactants can be capturing of toxic vapors or gases, which is essential for many industries where the by-product contains chlorine, sulfur, selenium, tellurium, nitrogen, phosphorus, arsenic, cadmium, mercury, thallium, lead, etc. (**Appendix A**). At the end of this kind of a process, it is enough to transfer the final solid product from the tribo-reactor into a regular container for subsequent storage in a sealed form.

### 4.3. Vacuum Insulated Windows

Currently, getter materials with a high sorption capacity are in demand from such products as vacuum windows, vacuum MEMS devices, vacuum insulated pipes, double gas pipes for laying in northern latitudes, etc. All of them are designed for long-term operation, they all use nondetachable types of hermetization and all have a specific vacuum cavity in the form of a geometric figure, in which one of the three dimensional parameters is incomparably smaller than the other two. Vacuum chambers of this kind experience all the weaknesses and disadvantages of getters adsorbents of the NEG class, their low sorption capacity and dependence on thermal activation.

The sorption capacity of the getters adsorbents is the higher the larger their specific surface area, *i.e.* the smaller the average size of the getter particles. However, the smaller these particles are, the less benefit from their thermal activation due to the growing ratio (volume of the passivated film)/(volume of the particle core) [59]. Besides, heating the getter in a sealed chamber with a narrow vacuum gap inevitably involves the walls of the chamber in this heating, which increases the gas load on the getter due to degassing of the wall.

Nevertheless, the main problem of vacuum chambers with a narrow internal gap, but a large total surface area, is the low specific sorption capacity of the adsorbents. It is proposed to solve this problem by using getters reactants with their outstanding sorption characteristics.

What vacuum windows are, how they are assembled, and what problems are holding back their mass production, are described in detail in a number of reviews [60] [61] [62] [63]. As shown in **Figure 21**, two glass plates 4 and 5 are hermetically connected at the edges with seal material 1, keeping these plates from collapsing with pillars 3. It is known that when a gap 6 between the plates is  $\sim 0.2$  mm, a high level of window thermal insulation is guaranteed if in the cavity a vacuum of the order of  $\sim 10^{-3}$  mbar is maintained. The task of the getter material is to maintain the specified pressure inside the window for many decades.

In the general case, the assembly is carried out in the following way (**Figure 21**). Getter material 2 is installed on plate 4 in normal atmosphere (Product 1),

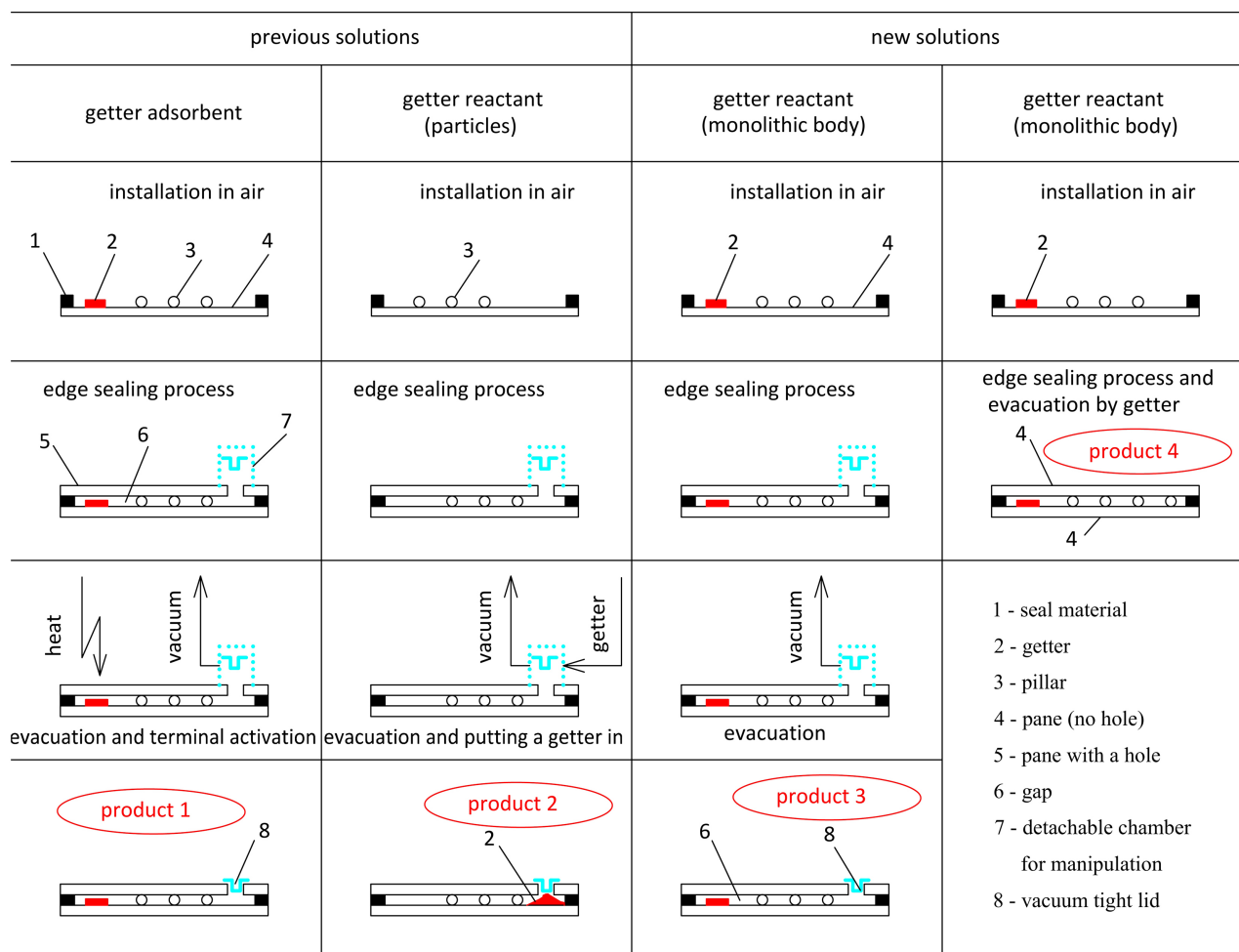


**Figure 21.** Scheme of a window assembly.

and then plate 5 is installed and the window is sealed along the edges. Alternatively, the getter is introduced into the window through detachable chamber 7 under vacuum (Product 2). In both cases, the assembly process ends with the sealing of the exhaust hole in the upper plate 5 with a plug 8 under vacuum. Examples of Product 1 are windows with getters of NEG type and/or Ba EGs [64], and examples of Product 2 are windows with getters reactants in granular form [5]. Windows with hybrid getters adsorbents [65] adjoin Product 2 according to the assembly scheme, but according to their properties, which are determined by the nature of the getter, they should be assigned to Product 1.

The disadvantages of Product 1 are the disadvantages of NEG getters, their need of thermal activation and negligible sorption capacity. Product 2 does not have these drawbacks; however, transporting the active metal material along the lines of the vacuum system is a risky operation. Therefore, the class of getters reactants was expanded due to macro-bodies with a monolithic structure, which have a temporary resistance to air, but further decompose under the action of gases to small particles already inside the window (Product 3).

A new technological option is to seal the window at the edges in air, without

using vacuum pumps (Product 4). Due to their extremely high sorption capacity, IIA metal alloys are able to replace the vacuum pump, chemically binding all gases except argon, which remains in the cavity between the plates as a residual gas at a pressure of about 10 mbar.

Following the assembly diagram for Product 4, one can replace the air between the plates with CO<sub>2</sub> before connecting them and seal the window around the edges with carbon dioxide inside. Upon completion of the reaction between CO<sub>2</sub> and the getter reactant, this window becomes an analogue of Product 3. You can go further and, before joining the plates, use a mixture of CO<sub>2</sub> and air in any given ratio to fill the cavity 6, which will allow regulating the Ar pressure in the gap according to the composition of the given gas mixture.

From the above, it can be seen that getters reactants give a chance to transform vacuum windows into a mass product with a long lifetime at low production costs. However, alloys of alkaline earth metals can also be used as getters in argon-filled windows [66] [67]. The quality of windows of this type is improved, and their service life increases when the standard desiccants based on zeolites are replaced with new desiccants with the addition of reactant getters (**Appendix B**).

## 5. Concluding Remarks

The present review discloses the sorption mechanism of getters reactants and provides an analysis of their prospects in the field of sorption technologies, based on the latest experimental data [10] [14]. As known, alloys of IIA metals in the form of highly porous bodies, powders and films are the most advantageous getter products in respect of sorption capacity. However, transferring such a highly active material from the place, where it is produced to the position, where it is used, is a technically challenging and a rather costly task. For getters of this class, even a short-term contact with air is unacceptable.

The problem was solved after numerous attempts, and not with the help of design or procedural developments, but quite unexpectedly by expanding the dimensional and structural boundaries of getters reactants, namely, by simply replacing films, powders, or porous bodies with the same reactive alloys in the form of macro-bodies with monolithic structure. This solution follows directly from the results of the studies.

According to the obtained data, the surface of cast samples of the reactive alloy in a gas medium is covered with a layer of products several microns thick, which stops the chemical reaction with gases and transfers the process to the incubation stage. This gives rise to the idea of a sacrificial layer, which greatly simplifies all operations for transferring and loading the getter product, which are now carried out in air.

At the same time, the main indicator of the sorption process, which is the degree of involvement of the getter material in the reaction with gases, is determined by the rate of corrosion decomposition of the reactive ingot. This decay is a new phenomenon in getter practice, and it was also discovered and recruited

for positive purposes in the mentioned works for the first time [10] [14]. Let us especially note that this corrosive decomposition, which feeds the sorption process with a fresh metal surface, proceeds in a gaseous medium not very fast and not very slowly, but within the very boundaries that allow it to be used in solving traditional sorption tasks.

The fact that the time law of corrosion destruction of an ingot depends not only on the gas load, but also on the composition of the ingot, its microstructure and the concentration of defects in it, deserves special mention. These three characteristics of the ingot are put into it at the production stage and can be pre-selected in such a way as to achieve the optimal agreement with the gas load.

So, a new modification of getters reactants in a form of macro-bodies with a monolithic structure is entering the arena of sorption technologies. These materials free us from the conventional production scheme, based *a priori* on highly porous materials with a carcass structure, which creates many problems due to their initial structure and conventional way of employing them. The new production order, established with the arrival of modified getters reactants, is simpler in implementation and more economical, and most importantly, more efficient in terms of sorption.

### Conflicts of Interest

The authors declare no conflicts of interest regarding the publication of this paper.

### References

- [1] Fransen, J.J.B. and Perdijk, H.J.R. (1960) The Absorption of Gases by Barium Getter Films Applied as a Tool. *Vacuum*, **10**, 199-203. [https://doi.org/10.1016/0042-207X\(60\)90136-6](https://doi.org/10.1016/0042-207X(60)90136-6)
- [2] Ferrario, B. (1998) Getters and Getter Pumps. In: Lafferty, J.M., Ed., *Foundation of Vacuum Science and Technology*, Wiley, New York, 261-290.
- [3] Ferrario, B. (1996) Chemical Pumping in Vacuum Technology. *Vacuum*, **47**, 363-370. [https://doi.org/10.1016/0042-207X\(95\)00252-9](https://doi.org/10.1016/0042-207X(95)00252-9)
- [4] Chuntonov, K., Ivanov, A.O., Verbitsky, B. and Kozhevnikov, V.L. (2017) Gas Purification and Quality Control of the End Gas Product. *Journal of Materials Science and Chemical Engineering*, **5**, 44-58.
- [5] Chuntonov, K., Ivanov, A.O., Verbitsky, B. and Setina, J. (2018) Getters for Vacuum Insulated Glazing. *Vacuum*, **155**, 300-306. <https://doi.org/10.1016/j.vacuum.2018.06.012>
- [6] Ropp, R.C. (2013) Encyclopedia of the Alkaline Earth Compounds. Elsevier, Amsterdam. <https://doi.org/10.1016/B978-0-444-59550-8.00001-6>
- [7] Chuntonov, K. and Lee, M.K. (2014) Mechanochemical Sorption Apparatuses. *Advanced Materials Research*, **875-877**, 1106-1110. <https://doi.org/10.4028/www.scientific.net/AMR.875-877.1106>
- [8] Chuntonov, K. and Setina, J. (2017) Activationless Gas Purifiers with High Sorption Capacity. US Patent 9586173. <https://patft.uspto.gov/netacgi/nph-Parser?Sect1=PTO2&Sect2=HITOFF&p=1&u=>

- [%2Fnethtml%2FPTO%2Fsearch-bool.html&r=8&f=G&l=50&co1=AND&d=PTXT&s1=chuntonov&OS=chuntonov&RS=chuntonov](#)
- [9] Chuntonov, K., Ivanov, A.O. and Kozhevnikov, V.L. (2020) Tribochemical Purification of Gases. I. The Process Model. *Journal of Materials Science and Chemical Engineering*, **8**, 37-54. <https://doi.org/10.4236/msce.2020.82005>
- [10] Chuntonov, K., Soloduha, E. and Yoffe, Y. (2020) Tribochemical Sorption Analyzer (IL Pat. Appl. 27545).
- [11] Mono Torr Heated Getter Gas Purifiers (2016) Brochure SAES Pure Gas. [http://www.saespuregas.com/Library/specifications-brochures/MonoTorr\\_Brochure.pdf](http://www.saespuregas.com/Library/specifications-brochures/MonoTorr_Brochure.pdf)
- [12] Entegris (2018) White Paper. Bowling for Contaminants: The New Science of Gas Purification. 1-7. <https://www.entegris.com/content/dam/web/resources/white-papers/whitepaper-bowling-for-contaminants-10071.pdf>
- [13] Entegris (2019) White Paper. Eliminating Unwanted Oxygen: Preventing Device Failure at the Source. 1-6. <https://info.entegris.com/eliminating-unwanted-oxygen-preventing-device-failure-at-the-source>
- [14] Chuntonov, K., Chuntonov, A. and Kozhevnikov, V.L. (2021) Vacuum Windows with Getter Reactants (IL Pat. Appl.285365).
- [15] Bosseboeuf, A., Lemette, S., Wu, M., Moulin, J., Coste, P., Bessouet, C., Hammami, S., Renard, C. and Vincent, L. (2019) Effect of Environment on Activation and Sorption of Getter Alloys and Multilayers for Hybrid Wafer-Level Vacuum Packaging. *Sensor and Materials*, **31**, 2825-2849. <https://doi.org/10.18494/SAM.2019.2312>
- [16] Chuntonov, K., Atlas, A., Setina, J. and Douglass, G. (2016) Getters: From Classification to Materials Design. *Journal of Materials Science and Chemical Engineering*, **4**, 23-34. <https://doi.org/10.4236/msce.2016.43004>
- [17] Littmann, M. (1938) Getterstoffe und ihre Anwendung in der Hochvakuumtechnik. CF Wintersche Veriagshandlung, Leipzig.
- [18] Chandrasekharaiah, M.S. and Margrave, J.L. (1961) Kinetics of Oxidation and Nitridation of Lithium, Calcium, Strontium and Barium. *Journal of the Electrochemical Society*, **108**, 1008-1012. <https://doi.org/10.1149/1.2427937>
- [19] Pirani, M. and Yarwood, J. (1961) Principles of Vacuum Engineering. Reinhold Publishing Corp., New York.
- [20] Turnbull, J.C. (1977) Barium, Strontium, and Calcium as Getter in Electron Tubes. *Journal of Vacuum Science and Technology A*, **14**, 636-639. <https://doi.org/10.1116/1.569166>
- [21] Chuntonov, K. and Setina, J. (2016) Reactive Getters for MEMS Applications. *Vacuum*, **123**, 42-48. <https://doi.org/10.1016/j.vacuum.2015.10.012>
- [22] Czaja, A.U., Trukhan, N. and Müller, U. (2009) Industrial Applications of Metal-Organic Frameworks. *Chemical Society Reviews*, **38**, 1284-1293. <https://doi.org/10.1039/b804680h>
- [23] Roth, W., Nachtigal, P., Morris, R., Wheatley, P.S., Seymour, V.R., Ashbrook, S.E., Chlubná, P., Grajciar, L., Položij, M., Zukal, A., Shvets, O. and Čejka, J. (2013) A Family of Zeolites with Controlled Pore Size Prepared Using a Top-Down Method. *Nature Chemistry*, **5**, 628-633. <https://doi.org/10.1038/nchem.1662>
- [24] Hönicke, I.M., Senkovska, I., Bon, V., Baburin, I.A., Bönisch, N., Raschke, S., Evans, J.D. and Kaskel, S. (2018) Balancing Mechanical Stability and Ultrahigh Porosity in

- Crystalline Framework Materials. *Angewante Chemie International Edition*, **57**, 13780-13783. <https://doi.org/10.1002/anie.201808240>
- [25] Seow, J.Y.R., Skinner, W.S., Wang, Z.U. and Jiang, H.-L. (2020) Metal-Organic Frameworks: Structures and Functional Applications. *Materials Today*, **27**, 43-68. <https://doi.org/10.1016/j.mattod.2018.10.038>
- [26] Teo, W.L., Zhou, W., Qian, C. and Zhao, Y. (2021) Industrializing Metal-Organic Frameworks: Scalable Synthetic Means and Their Transformation into Functional Materials. *Materials Today*, **47**, 170-186. <https://doi.org/10.1016/j.mattod.2021.01.010>
- [27] Boffito, C. and Schiabel, A. (1994) Process for the Sorption of Residual Gas by Means of a Non-Evaporated Barium Getter Alloy. US Patent 5,312,606.
- [28] Schiabel, A. and Boffito, C. (1994) Process for the Sorption of Residual Gas by Means of a Non-Evaporated Barium Getter Alloy. US Patent 5,312,607.
- [29] Ricca, F. and della Porta, P. (1960) Carbon Monoxide Sorption by Barium Films. *Vacuum*, **10**, 215-222. [https://doi.org/10.1016/0042-207X\(60\)90140-8](https://doi.org/10.1016/0042-207X(60)90140-8)
- [30] della Porta, P. and Argano, E. (1960) Nitrogen Sorption by Barium Films. *Vacuum*, **10**, 223-226. [https://doi.org/10.1016/0042-207X\(60\)90141-X](https://doi.org/10.1016/0042-207X(60)90141-X)
- [31] Giedraitis, A., Tamulevicius, S., Gudaitis, R., *et al.* (2010) Kinetics of Growth and Sorption Properties of Evaporable Barium Getter Films. *Materials Science (Medzia Gotyra)*, **16**, 12-23.
- [32] Verhoeven, J. and van Doveren, H. (1982) Interaction of Residual Gases with Barium Getter Film as Measured by AES and XPS. *Journal of Vacuum Science & Technology*, **20**, 64-74. <https://doi.org/10.1116/1.571310>
- [33] American Society for Testing and Materials, West Conshohocken, PA (1997) ASTM F798-97, Standard Practice for Determining Gettering Rate, Sorption Capacity, and Gas Content of Nonevaporable Getters in the Molecular Flow Region. (Reapproved 2002)
- [34] Young, D. (1966) *Decomposition of Solids*. Pergamon Press, Oxford.
- [35] Barret, P. (1973) *Cinetique Heterogene*. Gauthier-Villars, Paris.
- [36] Brown, W.E., Dollimore, D. and Galwey, A.K. (1980) Reactions in the Solid State. In: Bamford, C.H. and Tipper, F.H., Eds., *Comprehensive Chemical Kinetics*, Vol. 22, Elsevier, Amsterdam, 1-340.
- [37] Grimley, T.B. (1955) Oxidation of Metals. In: Garner, W.E., Ed., *Chemistry of Solid State*, Chapter 14, Butterworth, London, 336-366.
- [38] Low, M.J.D. (1960) Kinetics of Chemisorption of Gases on Solids. *Chemical Reviews*, **3**, 267-312. <https://doi.org/10.1021/cr60205a003>
- [39] Hauffe, K. (1965) *Oxidation of Metals*. Springer, Berlin.
- [40] Wise, H. and Oudar, J. (1990) *Material Concept in Surface Reactivity and Catalysis*. Academic Press, San Diego.
- [41] Rudzinski, W. (1997) A New Theoretical Approach to Adsorption-Desorption Kinetics on Energetically Heterogeneous Flat Solid Surface Based on Statistical Rate Theory of Interfacial Transport. In: Rudzinski, W., Steele, W.A. and Zgrablich, G., Eds., *Studies in Surface Science and Catalysis*, Elsevier, Amsterdam, Vol. 104, 335-371. [https://doi.org/10.1016/S0167-2991\(97\)80069-9](https://doi.org/10.1016/S0167-2991(97)80069-9)
- [42] Panczyk, T. and Rudzinski, W. (2004) Kinetics of Gas Adsorption on Strongly Heterogeneous Solid Surfaces: A Statistical Rate Theory Approach. *Korean Journal Chemical Engineering*, **21**, 206-211. <https://doi.org/10.1007/BF02705400>

- [43] Rudzinski, W., Panczyk, T. and Plazinski, W. (2005) Kinetics of Isothermal Gas Adsorption on Heterogeneous Solid Surfaces: Equations Based on Generalization of the Statistical Rate Theory of Interfacial Transport. *The Journal Chemistry B*, **109**, 21868-21878. <https://doi.org/10.1021/jp052671v>
- [44] Fontana, M.G. (1987) Corrosion Engineering. Third Edition, McGraw-Hill Book, Singapore.
- [45] Kaesche, H. (1990) Die Korrosion der Metalle: Physikalisch-chemische Prinzipien und aktuelle Probleme. Springer, Heidelberg.
- [46] Atrens, A., Winzer N., Dietzel, W., Srinivasan, P.B. and Song, G.-L. (2011) Stress Corrosion Cracking (SCC) of Magnesium (Mg) Alloys. In: Song, G.-L., Ed., *Corrosion of Magnesium Alloys*, Woodhead Publishing, London, 299-364. <https://doi.org/10.1533/9780857091413.3.299>
- [47] Kappens, M., Iannuzzi, M. and Carranza, R.M. (2013) Hydrogen Embrittlement of Magnesium and Magnesium Alloys: A Review. *Journal of the Electrochemical Society*, **160**, C168-C178. <https://doi.org/10.1149/2.023304jes>
- [48] Nagumo, M. (2016) Fundamentals of Hydrogen Embrittlement. Springer, Singapore. <https://doi.org/10.1007/978-981-10-0161-1>
- [49] McCarrol, I.E., Haley, D., Thomas, S., Meier, M.S., Bagot, P.A.J., Moody, M.P., Birbilis, N. and Cairney, J.M. (2020) The Effect of Hydrogen on the Early Stages of Oxidation of a Magnesium Alloy. *Corrosion Science*, **165**, Article ID: 108391. <https://doi.org/10.1016/j.corsci.2019.108391>
- [50] Okamoto, H. (2000) Phase Diagrams for Binary Alloys. ASM International, Materials Park.
- [51] Borgstedt, H.U. and Mathews, C.K. (1987) Applied Chemistry of the Alkali Metals. Plenum Press, New York.
- [52] Chuntonov, K. and Setina, J. (2008) New Lithium Gas Sorbents: I. The Evaporable Variant. *Journal of Alloys and Compounds*, **455**, 489-496. <https://doi.org/10.1016/j.jallcom.2007.01.158>
- [53] Chuntonov, K., Ivanov, A.O. and Permikin, D. (2009) New Lithium Gas Sorbents: IV. Application to MEMS Devices. *Journal Alloys and Compounds*, **471**, 211-216. <https://doi.org/10.1016/j.jallcom.2008.03.060>
- [54] Hart, C.A., Skinner, C.H., Capece, A.M. and Koel, B.E. (2016) Sorption of Atmospheric Gases by Bulk Lithium Metal. *Journal of Nuclear Materials*, **468**, 71-77. <https://doi.org/10.1016/j.jnucmat.2015.11.006>
- [55] Chuntonov, K., Verbitsky, B., Ivanov, A.O. and Kozhevnikov, V.L. (2018) Mechanochemical Methods in the Production of High Purity Gases. *Materials Sciences and Applications*, **9**, 489-501. <https://doi.org/10.4236/msa.2018.95034>
- [56] Janz, A. and Schmid-Fetzer, R. (2009) Thermodynamics and Constitution of Mg-Al-Ca-Sr-Mn Alloys: Part I. Experimental Investigation and Thermodynamic Modeling of Subsystems Mg-Ca-Sr and Al-Ca-Sr. *Journal of Phase Equilibria and Diffusion*, **30**, 146-156. <https://doi.org/10.1007/s11669-009-9467-4>
- [57] Aljarrah, M. and Medraj, M. (2008) Thermodynamic Modelling of the Mg-Ca, Mg-Sr, Ca-Sr and Mg-Ca-Sr Systems Using the Modified Quasichemical Model. *Calphad*, **32**, 240-251. <https://doi.org/10.1016/j.calphad.2007.09.001>
- [58] Elliott, R. (1983) Eutectic Solidification Processing. Crystalline and Glassy Alloys. Butterworths, London. <https://doi.org/10.1016/B978-0-408-10714-3.50007-1>
- [59] Chuntonov, K. and Yatsenko, S. (2013) Getter Films for Small Vacuum Chambers. *Recent Patent on Materials Science*, **6**, 29-39.

- <https://doi.org/10.2174/1874464811306010029>
- [60] Collins, R. (2019) Vacuum Insulating Glasses—Past, Present and Prognosis. <https://www.glassonweb.com/article/vacuum-insulating-glass-past-present-and-prognosis>
- [61] Kocer, C. (2020) The Past, Present, and Future of the Vacuum Insulated Glazing Technology. <https://www.glassonweb.com/article/past-present-and-future-vacuum-insulated-glazing-technology>
- [62] Park, J., Oh, M. and Lee, C.-S. (2019) Thermal Performance Optimization and Experimental Evaluation of Vacuum-Glazed Windows Manufactured via the In-Vacuum Method. *Energies*, **12**, 3634. <https://doi.org/10.3390/en12193634>
- [63] Zhang, S., Kong, M., Memon, S., Miao, H., Zhang, Y. and Liu, S. (2020) Thermal Analysis of a New Neutron Shielding Vacuum Multiple Glass. *Sustainability*, **12**, 3083. <https://doi.org/10.3390/su12083083>
- [64] Hogan, J.P., Pankte, A.W. and Petrmichl, R.H. (2016) Method of Making Vacuum Insulated Glass (VIG) Window Unit Including Activating Getter. US Patent 9,290,984.
- [65] Abe H., Uriu, E., Hasegawa, K., Ishibashi, T., Nonaka, M., Shimizu, T. and Ishikawa, H. (2021) Glass Panel Unit, Building Component, and Method for Activating Gas Adsorbent. US Patent 11,028,637.
- [66] van Den Bergh, S., Hart, R., Jelle, B.P. and Gustavsen, A. (2013) Window Spacers and Edge Seals in Insulating Glass Units: A State-of-the-Art Review and Future Perspectives. *Energy and Buildings*, **58**, 263-280. <https://doi.org/10.1016/j.enbuild.2012.10.006>
- [67] Respondek, Z. (2020) Heat Transfer through Insulating Glass Units Subjected to Climatic Loads. *Materials*, **13**, 286. <https://doi.org/10.3390/ma13020286>
- [68] von Schnering, H.G., Eisenmann, B. und Müller, W. (1973) Zintl Phases: Übergangsformen zwischen Metall- und Ionenbindung. *Angewandte Chemie*, **17**, 742-760. <https://doi.org/10.1002/ange.19730851704>
- [69] von Schnering, H.G. (1981) Homonucleare Bindungen bei Hauptgruppenelmenten. *Angewandte Chemie*, **93**, 44-63. <https://doi.org/10.1002/ange.19810930107>
- [70] Schäfer, H. (1985) On the Problem of Polar Intermetallic Compounds: The Stimulation of E. Zintl's Work for the Modern Chemistry of Intermetallics. *Annual Review of Materials Science*, **15**, 1-42. <https://doi.org/10.1146/annurev.ms.15.080185.000245>
- [71] Sevov, S.C. (2002) Zintl Phases. In: Westbrook, J.H. and Fleischer, R.L., Eds., *Intermetallic Compounds: Vol. 3, Principles and Practice*, John Wiley & Sons, Ltd., Hoboken 113-132. <https://doi.org/10.1002/0470845856.ch6>
- [72] Kauzlarich, S.M., Zevalkink, A., Toberer, E. and Snyder, G.J. (2017) Chapter 1: Zintl Phases: Recent Developments in Thermoelectrics and Future Outlook. In: *Thermoelectric Materials and Devices*, The Royal Society of Chemistry, London, 1-26. <https://doi.org/10.1039/9781782624042-00001>
- [73] Balvanz, A., Qu, J., Baranets, S., Elif, E., Gorai, P. and Bobev, S. (2020) New n-Type Zintl Phases for Thermoelectrics: Discovery, Structural Characterization, and Band Engineering of the Compounds A<sub>2</sub>CdP<sub>2</sub> (A = Sr, Ba, Eu). *Chemistry of Materials*, **32**, 10697-10707. <https://doi.org/10.1021/acs.chemmater.0c03960>

## Appendix A

The ability of IIA metals to form stable chemical compounds with N, P, As, S, Se, Cl, etc., or with substances containing them, which are often very aggressive to the environment, looks completely natural. However, a similar ability of IIA metals to form strong intermediate phases was found in relation to typical metals such as Cd, Zn, Hg, Tl, Pb. In these phases, called Zintl phases [68]-[73], the mentioned metals occupy the positions of a polyanion with internal covalent bonds, which leads to increased chemical and thermal stability of these compounds.

This gives rise to the idea of using getters reactants in operations for capturing and conservation of toxic waste containing both the mentioned metals and the above-listed elements of VA-VIIA groups. These wastes hazardous to the human body are by-products of such modern industries as pharmaceuticals, microelectronics, semiconductor or military industries, etc. And the best way to trap and neutralize harmful vapors and gases of this nature is to capture them with solid reactants in flow sorption traps, or in triboreactors of the type we have described [9] [10].

## Appendix B

The service life of glass units with argon filling can be extended by adding getters reactants in the form of perforated ribbons or simply granules to the zeolite-based dehumidifiers, which are currently used to trap moisture from the interior space. **Figure A1** shows a schematic cross-section of spacer with drying material (zeolites), in the middle of which a getter reactant is placed.

Getters reactants have two advantages over adsorbents. First, the water holding capacity of IIA metals is much higher than that of zeolites. Secondly, in zeolites, with a decrease in water vapor pressure, not only the rate of moisture trapping, but also the sorption capacity decreases, while in getters reactants, this last characteristic remains at the same high level.

Simple estimations based on sorption data on zeolites and IIA metals show that if the volume  $V_g$  of the getter additive is within the range  $0.1V \leq V_g \leq 0.2V$ , where  $V$  is the total volume of zeolite and the getter additive, then the moisture capacity of such a modernized desiccant increases at least not less than by 2 times. In the case of mass production of getters reactants the cost per unit of their volume will not exceed that for those zeolites that are used in double-glazed windows.

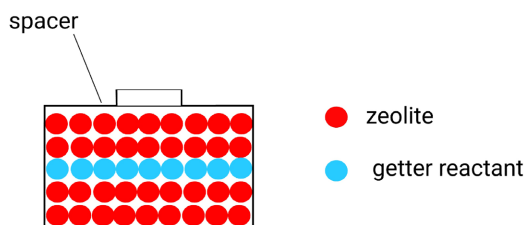


**Figure A1.** Spacer for argon-filled windows.